Uterine FK506-binding protein 52 (FKBP52)–peroxiredoxin-6 (PRDX6) signaling protects pregnancy from overt oxidative stress

Yasushi Hirota[a,b,1], Nuray Acar[a,c,1], Susanne Tranguch[a], Kristin E. Burnum[d], Huirong Xie[a], Ako Kodama[b], Yutaka Osuga[b], Ismail Ustunel[c], David B. Friedman[d], Richard M. Caprioli[d], Takiko Daikoku[a], and Sudhansu K. Dey[a,2]

[a]Division of Reproductive Sciences, The Perinatal Institute, Cincinnati Children's Hospital Medical Center, University of Cincinnati College of Medicine, Cincinnati, OH 45229; [b]Department of Obstetrics and Gynecology, University of Tokyo, Tokyo 113-8655, Japan; [c]Department of Histology and Embryology, School of Medicine, Akdeniz University, Antalya 07070, Turkey; and [d]Mass Spectrometry Research Center, Vanderbilt University Medical Center, Nashville, TN 37232

Edited by Bert W. O'Malley, Baylor College of Medicine, Houston, TX, and approved July 26, 2010 (received for review July 1, 2010)

Immunophilin FK506-binding protein 52 (FKBP52) is a cochaperone that binds to the progesterone receptor (PR) to optimize progesterone (P_4)-PR signaling. We recently showed that *Fkbp52*-deficient (*Fkbp52*$^{-/-}$) mice have reduced uterine PR responsiveness and implantation failure which is rescued by excess P_4 supplementation in a genetic background-dependent manner. This finding led us to hypothesize that FKBP52 has functions in addition to optimizing PR activity. Using proteomics analysis, we found that uterine levels of peroxiredoxin-6 (PRDX6), a unique antioxidant, are significantly lower in *Fkbp52*$^{-/-}$ mice than in WT and PR-null (*Pgr*$^{-/-}$) mice. We also found that *Fkbp52*$^{-/-}$ mice with reduced uterine PRDX6 levels are susceptible to paraquat-induced oxidative stress (OS), leading to implantation failure even with P_4 supplementation. The same dose of paraquat did not interfere with implantation in WT mice. Moreover, treatment with antioxidants α-tocopherol and N-acetylcysteine (NAC) attenuated paraquat-induced implantation failure in P_4-treated *Fkbp52*$^{-/-}$ mice. Functional analyses using mouse embryonic fibroblasts show that *Fkbp52* deficiency associated with reduced PRDX6 levels promotes H_2O_2-induced cell death, which is reversed by the addition of NAC or by forced expression of PRDX6, suggesting that *Fkbp52* deficiency diminishes the threshold against OS by reducing PRDX6 levels. These findings provide evidence that heightened uterine OS in *Fkbp52*$^{-/-}$ females with reduced PRDX6 levels induces implantation failure even in the presence of excess P_4. This study shows that FKBP52–PRDX6 signaling protects pregnancy from overt OS.

embryo implantation | mouse | uterus

Infertility is a global social and economic concern. It is estimated that by 2050 15% of couples worldwide will be childless because of infertility. Although many causes of infertility have been overcome by the application of in vitro fertilization and embryo transfer (IVF-ET), implantation failure is still a major obstacle for optimal pregnancy outcome. Pregnancy rates remain low in patients undergoing IVF-ET because of the transfer of embryos into a nonreceptive uterus, resulting in implantation failure (1). Heterogeneous uterine cell types respond differentially to estrogen and progesterone (P_4) to prepare the uterus to the receptive state. For successful implantation to occur, the uterus must be transiently receptive to implantation-competent blastocysts. P_4 signaling is an absolute requirement for implantation and pregnancy maintenance in most mammals studied (2). P_4 acts via the nuclear progesterone receptor (PR) to activate transcription of genes involved in ovulation, uterine receptivity, implantation, decidualization, and pregnancy maintenance (3).

We recently found that the immunophilin FK506-binding protein 52 (FKBP52) serves as a cochaperone to govern normal PR function in the mouse uterus, where its expression overlaps with that of PR. Immunophilins are so named because they bind to certain immunosuppressive drugs to mediate their actions. They are grouped into two families, FKBP and cyclosporin A-binding (cyclophilin, CyP) proteins. Some FKBP and CyP family members have a tetratricopeptide repeat (TPR) domain that targets binding to the conserved C terminus of Hsp90. FKBP52 is one such TPR-containing cochaperone that influences steroid hormone receptor function (4). The mature PR complex bound to FKBP52 binds to P_4 with high affinity and efficiency, although some basal PR responsiveness to P_4 is retained in the absence of FKBP52. In addition, FKBP52 plays a role in immunoregulation and basic cellular processes involving protein stability, folding, and trafficking (5–7).

We found that *Fkbp52*$^{-/-}$ females on both C57BL6/129 mixed and CD1 backgrounds have implantation failure with normal ovulation (8, 9). However, P_4 supplementation rescues implantation and decidualization in CD1, but not in C57BL6/129, *Fkbp52*$^{-/-}$ females. In CD1 *Fkbp52*$^{-/-}$ females, P_4 at higher-than-normal levels confers PR signaling sufficient for implantation, but even higher levels of P_4 are required to rescue full-term pregnancy (9). How P_4 overcomes reduced PR responsiveness to allow implantation in CD1 *Fkbp52*$^{-/-}$ mice is still unknown. Because FKBP52 positions PR in optimal conformation for binding to P_4, one possibility is that excess P_4 in the absence of FKBP52 increases the probability of random binding of P_4 to the PR complex even in its less optimal configuration. Alternatively, FKBP52 may influence other pathways along with PR signaling, because exogenous P_4 cannot rescue implantation in C57BL6/129 *Fkbp52*$^{-/-}$ mice and significantly higher P_4 levels are necessary to restore implantation and full-term pregnancy in CD1 *Fkbp52*$^{-/-}$ females (9). Moreover, *Fkbp52* also is expressed in the placenta with no detectable PR expression (9), implying that FKBP52 has other functions in addition to its role in optimizing PR activity. Our present study, using proteomics analysis, found that FKBP52 regulates oxidative stress (OS) by regulating the levels of a unique antioxidant, peroxiredoxin-6 (PRDX6), which operates independently of other peroxiredoxins and antioxidant proteins (10–12). Here we show that uterine FKBP52–PRDX6 signaling is a major player in countering the adverse effects of OS during early pregnancy.

Results

PRDX6 Levels Are Reduced in *Fkbp52*$^{-/-}$ Uteri. To explore downstream targets of FKBP52 independent of PR, we used proteomics approaches. Ovariectomized WT, *Fkbp52*$^{-/-}$, and PR-null (*Pgr*$^{-/-}$) mice on the C57BL6/129 background were treated with P_4 (2 mg/d) for 2 d, and uteri were collected 24 h after the second injection. Uterine protein lysates were subjected to 2D difference in gel electrophoresis (2D-DIGE) analysis with detection limits from 10- to 150-kDa proteins (pH 4–7) (Fig. 1*A*). Among the differentially expressed proteins, we found that PRDX6 levels are markedly down-regulated in *Fkbp52*$^{-/-}$ uteri compared with

Author contributions: Y.H., S.T., T.D., and S.K.D. designed research; Y.H., N.A., S.T., K.E.B., H.X., A.K., Y.O., D.B.F., and T.D. performed research; R.M.C. contributed new reagents/analytic tools; Y.H., N.A., S.T., I.U., T.D., and S.K.D. analyzed data; and Y.H., S.T., T.D., and S.K.D. wrote the paper.

The authors declare no conflict of interest.

This article is a PNAS Direct Submission.

[1]Y.H. and N.A. contributed equally to this work.

[2]To whom correspondence should be addressed. E-mail: sk.dey@cchmc.org.

This article contains supporting information online at www.pnas.org/lookup/suppl/doi:10.1073/pnas.1009324107/-/DCSupplemental.

$Pgr^{-/-}$ and WT uteri, with the exception of FKBP52, serving as an internal control (Table S1 and Fig. 1*B*). This finding led us to focus on PRDX6 as a potential downstream mediator of FKBP52 function, independent of its PR cochaperone activity, and to assess uterine expression of *Prdx6* in early pregnancy. Notably, we found that levels of six proteins increased in $Fkbp52^{-/-}$ uteri compared with WT uteri, but no differences were detected between WT and $Pgr^{-/-}$ uteri (Table S2). We confirmed down-regulated PRDX6 protein levels in $Fkbp52^{-/-}$ uteri compared with $Pgr^{-/-}$ and WT uteri by Western blotting (Fig. 1 *C* and *D*) and immunohistochemistry (Fig. 1*E*). In addition, both stromal and epithelial localization of PRDX6 was reduced in ovariectomized $Fkbp52^{-/-}$ uteri treated with P_4 (Fig. 1*E*).

To examine the effects of ovarian hormones on *Prdx6* expression in mouse uteri, we performed Northern and in situ hybridization using uteri from ovariectomized WT mice. Neither P_4 nor estradiol-17β (E_2) significantly altered *Prdx6* expression levels (Fig. S1*A*), but P_4 changed the expression domain from the epithelium to the stroma (Fig. S1*B*).

PRDX6 Is Aberrantly Expressed in $Fkbp52^{-/-}$ Uteri. On day 4 of pregnancy the uterus is under the influence of P_4 produced by the newly formed corpus luteum. PRDX6 is localized in both the stroma and epithelium in WT CD1 mice on day 4 of pregnancy (Fig. 1*F*). In contrast, in $Fkbp52^{-/-}$ uteri PRDX6 is restricted primarily to the epithelium but is localized in the subluminal stroma after P_4 supplementation (Fig. 1*F*). These results suggest that FKBP52 deficiency attenuates PRDX6 levels in the stroma that are compensated to some extent by P_4.

PRDX6 Is Differentially Expressed in Uteri During Early Pregnancy. The uterus is under the influence of preovulatory estrogen with increased epithelial cell proliferation on day 1 of pregnancy. On day 4, the uterus is exposed to heightened P_4 levels along with a small amount of estrogen, resulting in epithelial cell differentiation with stromal cell proliferation. The first molecular and physical interaction between the blastocyst and receptive uterus is observed on the evening of day 4, and the attachment process continues through day 5. The attachment reaction coincides with increased stromal vascular permeability solely at the site of the blastocyst and can be demarcated by distinct blue bands along the uterus after i.v. injection of a blue dye solution (13). The proliferating stromal cells surrounding the implanting blastocyst start to differentiate to decidual cells in the afternoon of day 5. Differentiating stromal cells in the immediate vicinity of the implanting blastocyst begin to form the primary decidual zone (PDZ) at this time. The PDZ is well formed on day 6 with the beginning of a proliferating secondary decidual zone (SDZ). Although cell proliferation ceases in the PDZ, it continues in the SDZ. The PDZ progressively degenerates as pregnancy progresses. On day 8, the implantation process is well advanced with maximal decidualization. We assessed *Prdx6* expression on days 1, 4, 5, and 8 of pregnancy by in situ hybridization. We found that *Prdx6* is detected mostly in the luminal epithelium on day 1 (Fig. 2*A*). On day 4, the expression is restricted to the stroma (Fig. 2*A*). *Prdx6* expression on these days closely resembles that of *Fkbp52* (14). On day 5, *Fkbp52* and *Prdx6* are expressed in a similar fashion in the decidualizing stroma surrounding the implanting blastocyst (Fig. 2 *A* and *B*). This overlapping expression of *Fkbp52* and *Prdx6* surrounding the implanting blastocyst suggests that the process of implantation may regulate these two molecules. On day 8, *Prdx6* is expressed primarily in the SDZ cells and in the embryo. PRDX6 protein levels also are up-regulated in uteri on days 5 and 8 of pregnancy (Fig. 2 *C* and *D*). In the placenta, *Fkbp52* and *Prdx6* showed a similar expression pattern in the labyrinth layer (Fig. 2*B*), with undetectable levels of PR (9). The similar localization of FKBP52 and PRDX6 in the deciduum and placenta suggests their PR-independent roles in these tissues. Furthermore, pull-down assays show that FKBP52 is physically

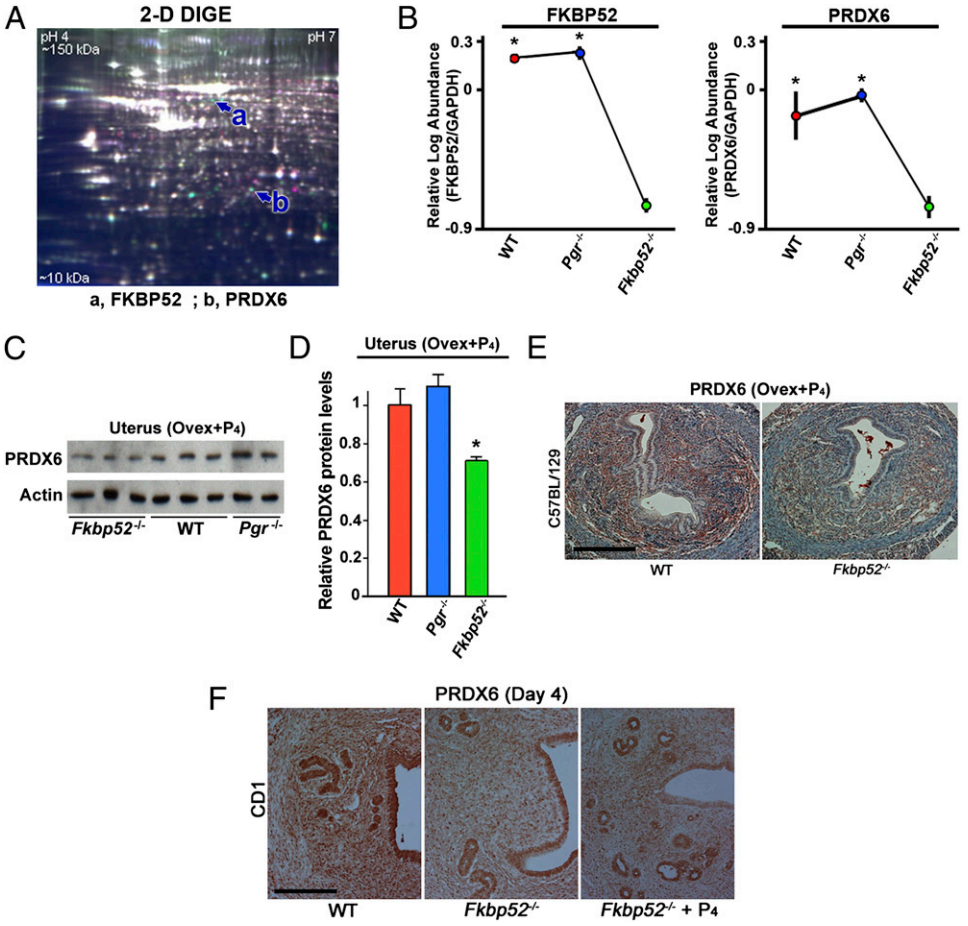


Fig. 1. PRDX6 expression is reduced in uteri of $Fkbp52^{-/-}$ mice. (*A*) A representative DIGE gel comprising protein extracts from WT and $Fkbp52^{-/-}$ uteri shows proteins of isoelectric points between pH 4–7 and apparent molecular mass between 10–150 kDa. a, FKBP52; b, PRDX6. (*B*) Decreased protein levels of PRDX6 and FKBP52 in P_4-treated uteri of $Fkbp52^{-/-}$ ovariectomized mice (n = 4) compared with WT (n = 3) and $Pgr^{-/-}$ (n = 3) ovariectomized mice on a C57BL6/129 background. Values are mean ± SEM. $^*P <$ 0.05 compared with $Fkbp52^{-/-}$ mice. (*C* and *D*) Decreased PRDX6 protein levels in P_4-treated uteri of $Fkbp52^{-/-}$ ovariectomized mice compared with WT and $Pgr^{-/-}$ ovariectomized females as determined by Western blotting. Band intensities are normalized against actin and expressed as relative ratios compared with WT samples on the C57BL6/129 background. Values are mean ± SEM of two or three independent samples. $^*P < 0.05$ compared with WT mice. (*E*) Differential expression patterns of PRDX6 protein in P_4-treated ovariectomized mouse uteri of WT and $Fkbp52^{-/-}$ mice on the C57BL6/129 background. (Scale bar, 200 μm.) (*F*) Differential expression patterns of PRDX6 protein in day 4 uteri of WT and $Fkbp52^{-/-}$ mice on a CD1 background. (Scale bar, 200 μm.)

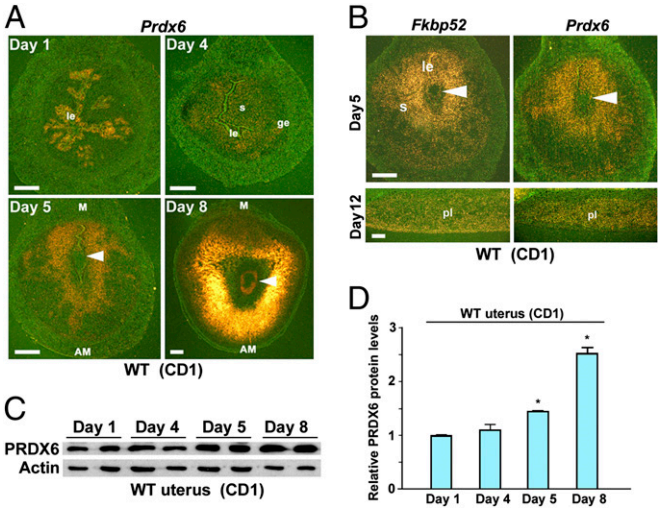


Fig. 2. Uterine PRDX6 is expressed differentially during early pregnancy. (*A*) In situ hybridization showing spatiotemporal expression of *Prdx6* in WT CD1 uteri on days 1, 4, 5, and 8 of pregnancy. Arrowheads indicate implanting embryos. AM, antimesometrial pole; ge, glandular epithelium; le, luminal epithelium; M, mesometrial pole; s, stroma. (Scale bar, 200 μm.) (*B*) Overlapping expression of *Fkbp52* and *Prdx6* in CD1 WT uteri on days 5 and 12 of pregnancy. Arrowheads indicate implanting embryos. le, luminal epithelium; pl, placenta; s, stroma. (Scale bars, 200 μm.) (*C* and *D*) Levels of uterine PRDX6 protein during early pregnancy as determined by Western blotting. Band intensities of PRDX6 were normalized against actin. Two independent samples from different mice were examined in each group. Data are expressed as mean ± SEM. $*P < 0.05$ compared with day 1 uteri.

associated with PRDX6 in the deciduum (Fig. S2), suggesting that FKBP52 influences PRDX6 status through this interaction.

In the human endometrium, both PRDX6 and FKBP52 are expressed in epithelial cells during the proliferative phase and in both epithelial and stromal cells in the secretory phase (Fig. S3*A*). The higher levels of *Prdx6* in the secretory (receptive) phase suggest that uterine PRDX6 also plays antioxidant roles in human implantation (Fig. S3*B*).

***Fkbp52*$^{-/-}$ Uteri Are More Prone to Overt OS During Implantation.** Because PRDX6 levels are reduced in *Fkbp52*$^{-/-}$ uteri on day 4 of pregnancy, especially in the stroma (Fig. 1*F*), we speculated that *Fkbp52*$^{-/-}$ uteri are more susceptible to OS during implantation. We have shown previously that P_4 levels are comparable in WT and *Fkbp52*$^{-/-}$ mice. However, excess P_4 supplementation that markedly elevates circulating P_4 levels is required for implantation in *Fkbp52*$^{-/-}$ females (9). Although P_4 supplementation rescues implantation failure in CD1 *Fkbp52*$^{-/-}$ mice (9), concomitant administration of the OS-inducing agent paraquat (15 or 20 mg/kg) prevented this rescue (Table 1 and Fig. 3*A*). In contrast, similar doses of paraquat failed to affect implantation in WT mice (Table 1 and Fig. 3*A*). To minimize the detrimental effects of paraquat on embryo growth and activation, we also performed embryo-transfer experiments. Day 4 WT blastocysts were transferred into day 4 WT or P_4-treated *Fkbp52*$^{-/-}$ recipients that received paraquat 7 h before the embryo transfer. Again, *Fkbp52*$^{-/-}$ mice had reduced numbers of implantation sites, whereas WT recipients showed normal implantation when examined on day 5 (Table 2). It is interesting that even a smaller dose of paraquat (2 mg/kg) inhibited implantation in P_4-treated *Fkbp52*$^{-/-}$ mice (Table 3). These results suggest that *Fkbp52*$^{-/-}$ mice are quite prone to OS in the context of implantation. More interestingly, a combined treatment of two antioxidants, N-acetylcysteine (NAC) and α-tocopherol (αTCP), significantly attenuated paraquat-induced implantation failure in P_4-treated *Fkbp52*$^{-/-}$ mice (Table 3), indicating the contribution of OS to implantation failure. Our speculation that *Fkbp52*$^{-/-}$ mice are sensitive to OS is supported by the finding of higher levels of bound 8-isoprostane, a lipid peroxidation marker, in C57BL6/129 *Fkbp52*$^{-/-}$ uteri than in WT uteri on day 4 of pseudopregnancy (Fig. 3*B*).

***Fkbp52*$^{-/-}$ Mouse Embryonic Fibroblasts with Reduced PRDX6 Levels Are Susceptible to OS.** Because PRDX6 protects cells from membrane damage associated with phospholipid peroxidation, we speculated that reduced PRDX6 would reduce cell viability if challenged with overt OS. Indeed, in vitro studies with WT and *Fkbp52*$^{-/-}$ mouse embryonic fibroblasts (MEFs) show that FKBP52 deficiency is associated with reduced PRDX6 levels (Fig. 3*C*) and enhances H_2O_2-induced cell death (Fig. 3*D*). This adverse effect in *Fkbp52*$^{-/-}$ MEFs was reversed substantially by supplementation of NAC (Fig. 3*E*) and, more importantly, by forced expression of PRDX6 (Fig. 3 *E* and *F*), suggesting that *Fkbp52* deficiency lowers the threshold against reactive oxygen species (ROS) by reducing PRDX6 levels. Because PR expression is undetectable in these MEFs (Fig. S4), these results provide evidence for FKBP52's role independent of PR function.

Discussion

The highlight of the present study is that *Fkbp52*$^{-/-}$ uteri are susceptible to OS because of reduced PRDX6 levels. Although further investigation is warranted to explore the mechanism by which FKBP52 regulates PRDX6 levels, our observation of physical interaction between FKBP52 and PRDX6 suggests that FKBP52 stabilizes PRDX6 protein and attenuates its degradation as a function of its chaperone activity. FKBP52's roles in protein stability, folding, and trafficking have been reported previously (5–7).

The reduced tolerance to OS in *Fkbp52*$^{-/-}$ mice results in paraquat-induced failure of implantation and higher levels of ROS generation in the uterus. Because excess P_4 cannot prevent implantation failure in the face of overt OS induced by paraquat in CD1 *Fkbp52*$^{-/-}$ females, we believe that FKBP52 regulates OS, in addition to its function in optimizing PR activity and other potential functions. In fact, FKBPs have several physiological roles, including binding and sequestration of calcineurin, protein folding and assembly, protein trafficking, and direct regulation of protein activity (15). Our present study adds another function to the list of various activities that have been reported for FKBP52.

Table 1. Paraquat adversely affects implantation in *Fkbp52*$^{-/-}$ mice

Genotype	Paraquat (mg/kg)	No. of mice	No. of mice with IS (%)	No. of IS	No. of blastocysts recovered
WT	15	7	7 (100%)	12.1 ± 1.7	N/A
	20	7	7 (100%)	12.0 ± 0.7	N/A
Fkbp52$^{-/-}$ + P_4	0	8	8 (100%)	10.6 ± 0.6	N/A
	15	7	2 (29%)*	12.0 ± 2.3	25†
	20	5	1 (20%)*	5.0	17‡

WT and *Fkbp52* $^{-/-}$ females on a CD1 background were mated with CD1 WT fertile males, and the number of implantation sites (IS) was examined on day 5 of pregnancy. *Fkbp52*$^{-/-}$ females were treated with P_4 (2 mg/d) on days 2–4 of pregnancy. Paraquat was injected on day 4. Uteri without IS were flushed with saline to recover any unimplanted blastocysts. Values are mean ± SEM.
$*P < 0.05$ compared with WT mice treated with the same dose of paraquat; Student's *t* test. N/A = not applicable.
†Twenty-five blastocysts were recovered from five mice.
‡Seventeen blastocysts were recovered from four mice.

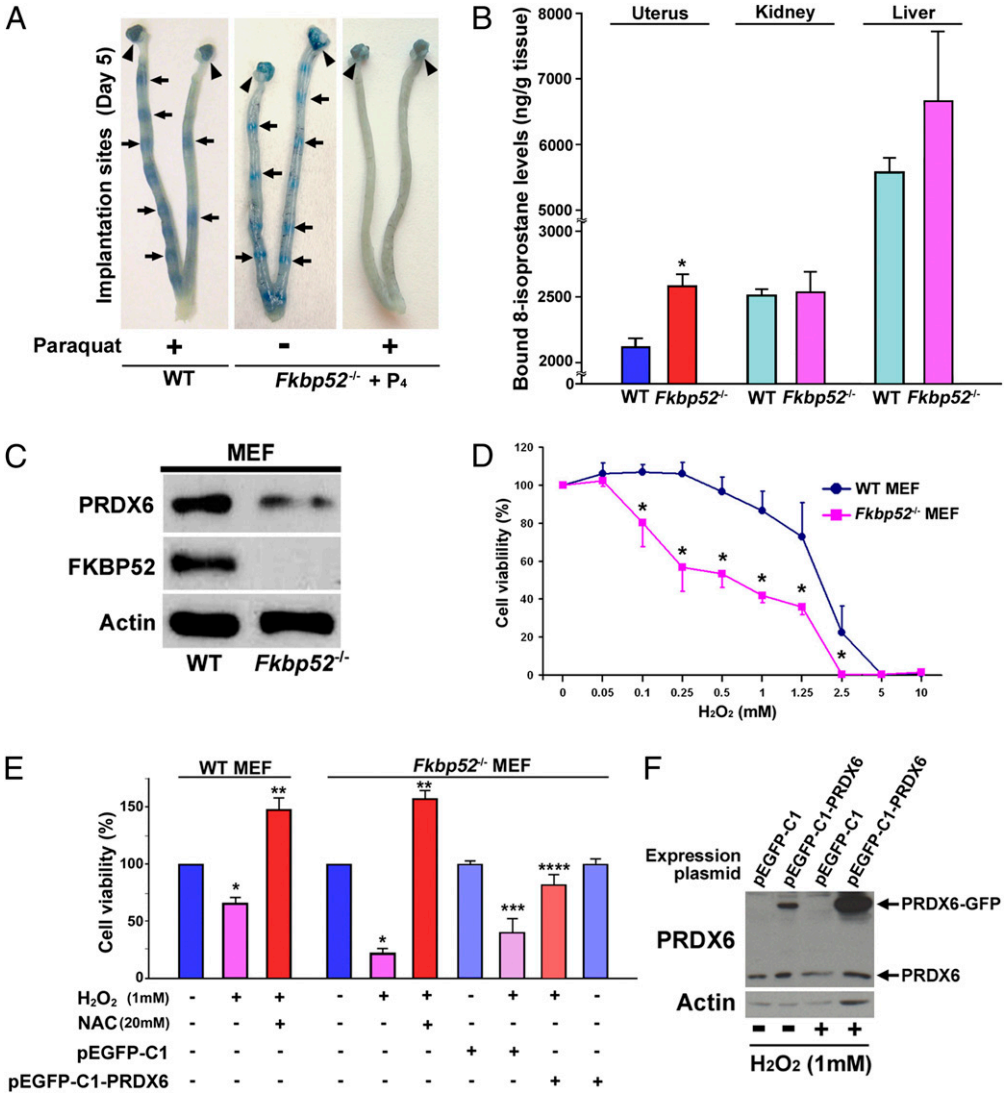


Fig. 3. *Fkbp52*$^{-/-}$ uteri are more prone to OS. (*A*) OS inducer paraquat blocks embryo implantation in P_4-primed CD1 *Fkbp52*$^{-/-}$ females on day 5 of pregnancy, whereas paraquat-treated CD1 WT uteri have normal numbers of implantation sites as demarcated by blue bands. *Fkbp52*$^{-/-}$ females were treated with P_4 (2 mg/d) on days 2–4 of pregnancy. Paraquat was injected on day 4. Arrows and arrowheads indicate implantation sites and ovaries, respectively. (*B*) Increased levels of bound 8-Isoprostane, a lipid peroxidation marker, in C57BL6/129 *Fkbp52*$^{-/-}$ uteri on day 4 of pseudopregnancy. Values are mean ± SEM of three independent samples. *$P < 0.05$ compared with WT mice. (*C*) Decreased levels of PRDX6 in *Fkbp52*$^{-/-}$ MEFs. Actin was used as a loading control. (*D*) Heightened sensitivity of *Fkbp52*$^{-/-}$ MEFs to H_2O_2-induced OS. Cells were treated with different concentrations of H_2O_2 for 24 h, and cell viability was evaluated by MTT assay. Values are mean ± SEM of six replicates from three independent experiments. *$P < 0.05$ compared with WT mice. (*E*) H_2O_2-induced cell death in *Fkbp52*$^{-/-}$ MEFs is protected by addition of NAC and forced expression of PRDX6. Cell viability was evaluated by MTT assay. Values are mean ± SEM of six replicates from three independent experiments. *$P < 0.05$, compared with vehicle-treated cells derived from mice of the same genotype. **$P < 0.05$, compared with H_2O_2-treated cells derived from mice of the same genotype. ***$P < 0.05$, compared with *Fkbp52*$^{-/-}$ cells transfected with pEGFP-C1 control plasmids; ****$P < 0.05$ compared with H_2O_2-treated *Fkbp52*$^{-/-}$ cells with transfection of pEGFP-C1 control plasmids. (*F*) PRDX6-GFP fused protein is induced effectively by transfection of pEGFP-C1-PRDX6 plasmids in *Fkbp52*$^{-/-}$ MEFs. pEGFP-C1 is a control plasmid.

PRDX6 is a unique nonredundant antioxidant that acts independently of other PRDXs and antioxidant enzymes (10–12). A recent study shows that *Prdx6*-deficient (*Prdx6*$^{-/-}$) mice have normal development, but paraquat-induced OS causes abnormal phenotypes such as lower survival rate, again not resulting from changes in gene expression and/or activity of other antioxidant enzymes (12). Thus, PRDX6 might be a critical antioxidant against exogenous OS. Our present finding of increased susceptibility of *Fkbp52*$^{-/-}$ uteri to OS during implantation because of reduced PRDX6 levels underscores the importance of uterine FKBP52–PRDX6 signaling during the periimplantation period. Although *Prdx6*$^{-/-}$ females were reported to be fertile (12), it is possible that exposure to OS will impair fertility in these mice. Indeed, it is known that certain genes serve critical functions during physiologically altered conditions. For example, deficiency of prolactin (PRL)-like protein A (PLP-A), a nonclassical member of the PRL family expressed in the mouse placenta, has little effect on female fertility under normal conditions, but PLP-A mutants show compromised pregnancy when exposed to a stressor (16). Thus, fertility in *Prdx6*$^{-/-}$ females could be compromised if PRDX6 deficiency is superimposed with OS. Future studies are warranted to characterize the female fertility phenotype in *Prdx6*$^{-/-}$ mice in a more systematic manner under normal and OS conditions. Collectively, our observations suggest that implantation failure in *Fkbp52*$^{-/-}$ mice not only is caused by the reduced PR activity but also is compounded by increased OS levels.

There is evidence that smoking and alcohol consumption reduce fertility in women by elevating OS (17, 18). Evidence also indicates that dietary antioxidant and diet-related exposures to ROS affect the timing and maintenance of pregnancy (19). These

Table 2. Paraquat inhibits implantation of transferred WT blastocysts in *Fkbp52*$^{-/-}$ recipients

Genotype of blastocysts	Genotype of recipients	Paraquat (mg/kg)	No. of blastocysts transferred	No. of recipients	No. of mice with IS (%)	No. of IS (%)	No. of blastocysts recovered
WT	WT	15	77	6	6 (100%)	58/77 (75%)	N/A
WT	*Fkbp52*$^{-/-}$+P_4	15	60	5	1 (20%)	1/60 (2%)	30*

Day 4 CD1 WT blastocysts were transferred into uteri of CD1 WT or CD1 *Fkbp52*$^{-/-}$ recipients on day 4 of pseudopregnancy. *Fkbp52*$^{-/-}$ recipients were treated with P_4 (2 mg/d) on days 2–4 of pregnancy. Paraquat was injected into the recipients 5 h before embryo transfer on day 4 of pregnancy. Uteri without IS were flushed with saline to recover any unimplanted blastocysts. N/A, not applicable.
*Thirty blastocysts were recovered from four mice.

findings, together with our observation that commercial rodent diets influence uterine gene expression and the timing of implantation in mice (20), suggest the possibility of ROS-induced alterations in uterine functions related to implantation. Because *Prdx6* is expressed primarily in the stroma in WT uteri on day 4 of pregnancy, the reduction of stromal *Prdx6* in *Fkbp52*$^{-/-}$ uteri even with P_4 supplementation may attenuate stromal function more drastically when exposed to OS. *Hoxa10* and *Ihh* are expressed in the stroma and epithelium, respectively, in day 4 pregnant mouse uteri (21, 22). Our results show that paraquat down-regulates *Hoxa10* expression without altering *Ihh* expression in *Fkbp52*$^{-/-}$ uteri (Fig. S5). In this respect, stromal *Prdx6* could be more important in protecting the uterus from overt OS and allowing implantation to proceed. Interestingly, we found a similar expression pattern of PRDX6 and FKBP52 in human endometrium and higher expression of *Prdx6* during the secretory phase, suggesting that these proteins may have physiological roles in human endometrium and implantation. It will be interesting to see whether endometria from patients with recurrent implantation failure have higher ROS because of low PRDX6 levels.

During the periimplantation period, embryos are exposed to low oxygen tension (23). Because preimplantation embryos are sensitive to OS (24), it is believed that a low oxygen condition is conducive to normal embryonic growth and development. This notion is consistent with the finding that antioxidants prevent ROS-induced abnormal embryo growth in culture (25, 26). Thus, the embryonic environment facing excess OS interferes with successful implantation. It also is a distinct possibility that the uterine environment is hypoxic during the periimplantation period to protect embryos from OS. Our findings that WT, but not *Fkbp52*$^{-/-}$, pregnant females treated with paraquat have normal implantation suggest that the uterus has a built-in protective system to combat OS to a degree and that PRDX6 is a critical player in this system. With increased angiogenesis after implantation, oxygen tension in the uterus and placenta increases, gradually exposing the developing embryo to higher ROS levels. Because a major role of the deciduum and placenta is to accommodate and protect the growing embryos, our data showing strong expression of *Prdx6* in these tissues in WT mice suggest that decidual and placental PRDX6 has an antioxidant function and protects embryos against increased oxygen tension at that time.

Endometriosis, the growth of endometrium-like tissues outside the uterus, is a common gynecological disease often associated with pelvic pain and infertility (27). Accumulating evidence shows that OS is associated with the pathogenesis of endometriosis and endometriosis-related infertility including implantation failure (28). Because our recent study has shown that FKBP52 levels are down-regulated in endometria of women with endometriosis compared with women without endometriosis (29), reduced FKBP52 levels may lead to endometrial PRDX6 deficiency, increasing uterine susceptibility to ROS, aggravating endometriosis, and adversely affecting endometrial receptivity in patients with endometriosis.

In conclusion, we show here that uterine FKBP52–PRDX6 signaling is a key player against ROS during pregnancy, an intriguing finding regarding a role of FKBP52–PRDX6 in uterine biology in the context of implantation.

Materials and Methods

Mice. C57BL/6/129 and CD1 *Fkbp52*$^{-/-}$ mice (9, 30) and C57BL6/129 *Pgr*$^{-/-}$ mice (31) were used in this study. FKBP52 and PR mutant mice were originally obtained from David Smith (Mayo Clinic, Scottsdale, AZ) and Bert O'Malley (Baylor College of Medicine, Houston, TX), respectively. All protocols for the present study were reviewed and approved by the Cincinnati Children's Research Foundation Institutional Animal Care and Use Committee.

Analysis of Implantation and Blastocyst Transfer. Mice were examined for implantation as described previously (9). WT and *Fkbp52*$^{-/-}$ females (2- to 5-mo-old) were mated with WT fertile males to induce pregnancy (day 1 = vaginal plug). To supplement *Fkbp52*$^{-/-}$ females with exogenous P_4, they were given an s.c. injection of P_4 (2 mg/d, s.c.) on days 2–4 of pregnancy. For induction of OS, paraquat was given i.p. to WT or *Fkbp52*$^{-/-}$ mice on day 4 (0900 hours) of pregnancy. For antioxidant treatment, NAC (50 mg/kg body weight) and αTCP (1g/kg body weight) were given i.p. daily on days 2–4. Pregnant females were killed on day 5 (0900 hours), and implantation sites were evaluated by i.v. injection of a Chicago blue dye solution. Uteri without implantation sites were flushed with saline to recover any unimplanted blastocysts. For blastocyst transfer experiments, pseudopregnant recipients were generated by mating females with vasectomized males. Paraquat was injected into recipients 5 h before embryo transfer on day 4 (0700 hours) of pregnancy. Day-4 WT blastocysts were transferred into day 4 uteri of WT or *Fkbp52*$^{-/-}$ pseudopregnant recipients (1200 hours), and implantation sites were examined 24 h later (day 5, 1200 hours).

Treatment with P_4 and/or E_2. To assess the effects of ovarian hormones on uterine *Prdx6* expression, CD1 WT females were ovariectomized and rested for 2 wk. They then were given a single s.c. injection of P_4 (2 mg) and/or E_2 (100 ng) (32). The control group of mice received only the vehicle (oil). Mice were killed after 24 h, and uteri were collected for Northern and in situ hybridization.

Human Tissues. Endometrial tissues were obtained from 24 women who had shown regular menstrual cycles without any hormonal treatment for at least 6 months. Endometrial samples were dated according to the women's

Table 3. Reversal of paraquat-induced implantation failure by treatment of antioxidants

Genotype	Paraquat (2 mg/kg)	NAC + αTCP	No. of mice	No. of mice with IS (%)	No. of IS (mean ± SEM)	No. of blastocysts recovered
Fkbp52$^{-/-}$ + P_4	+	–	10	1 (10%)	13.0	35†
	+	+	8	5 (63%)*	6.2 ± 1.7	22‡

Mice were given an i.p. injection of paraquat on day 4 of pregnancy. P_4 (2 mg/d) was administrated s.c. into each CD1 *Fkbp52*$^{-/-}$ mouse on days 2–4. NAC (50 mg/kg) and α-tocopherol (αTCP) (1 g/kg) were injected i.p. on days 2–4. Mice were killed on day 5, and their IS were examined by the blue dye method.
*$P < 0.05$ compared with *Fkbp52*$^{-/-}$ mice treated with the same dose of paraquat, P_4; Student's *t* test.
†Thirty-five blastocysts were recovered from nine mice.
‡Twenty-two blastocysts were recovered from three mice. Dormant-looking blastocysts were recovered from mice in which blue bands were not present or were very weak.

menstrual history and standard histological criteria (33). The experimental procedures were approved by the institutional review board of the University of Tokyo, and signed informed consent for the use of tissues was obtained from each woman.

2D-DIGE Analysis and Protein Identification. WT, *Fkbp52*$^{-/-}$, and *Pgr*$^{-/-}$ mice on C57BL6/129 background were ovariectomized, rested for 2 wk, and then treated daily with P_4 (2 mg) for 2 d. Mice were killed 24 h after the second P_4 injection, and their ueri were collected and processed for 2D-DIGE. Proteins were extracted from uterine tissues from three independent WT and *Pgr*$^{-/-}$ mice and four *Fkbp52*$^{-/-}$ mice, and 2D-DIGE and protein identification were performed as previously described by us (*SI Materials and Methods*) (14).

Immunoblotting. Protein extraction and Western blotting were performed as described (14). Antibodies to PRDX6, FKBP52 (kindly provided by Marc B. Cox, University of Texas, El Paso, TX), and actin were used. Actin served as a loading control.

Immunohistochemistry. Immunostaining of PRDX6 was performed in formalin-fixed paraffin-embedded sections using a specific antibody to PRDX6 (kindly provided by Aron B. Fisher, University of Pennsylvania, Philadelphia).

In Situ Hybridization. Paraformaldehyde-fixed frozen sections were hybridized with ^{35}S-labeled cRNA probes as described (13).

Northern Hybridization. Northern blotting was performed as described previously (13). *Rpl7* served as a housekeeping gene.

Immunoprecipitation. Decidual cells were isolated as described previously (34). Protein lysates were immunoprecipitated with an anti-FKBP52 antibody, and complexes were run on SDS/PAGE and immunoblotted using antibodies specific to PRDX6 or FKBP52. The control immunoprecipitation was performed by incubating the lysates with rabbit IgG.

Quantitative PCR. Quantitative PCR was performed as previously described (29). A housekeeping gene *Gapdh* was used as an internal standard.

RT-PCR. RT-PCR was performed as previously described (14). *Actb* served as a housekeeping gene.

8-Isoprostane Assay. Tissue levels of 8-isoprostane were assayed as described previously (35).

Isolation and Culture of MEFs. WT and *Fkbp52*$^{-/-}$ MEFs (kindly provided by Marc B. Cox, University of Texas, El Paso, TX) were isolated as described previously (8). The cells were maintained in DMEM supplemented with 10% FBS and penicillin/streptomycin.

MTT Assays. MEFs were cultured for 24 h in DMEM containing various concentrations of H_2O_2, and cell viability was determined with MTT assay as described previously (Promega) (36). To examine the effects of NAC on H_2O_2-induced cell damage, MEFs were pretreated with NAC for 24 h and then were treated with H_2O_2. To examine the effects of PRDX6 on H_2O_2-induced cell damage, *Fkbp52*$^{-/-}$ MEFs were transiently transfected with pEGFP-C1 (control vector carrying GFP alone, Clontech) or pEGFP-C1-PRDX6 (carrying GFP-PRDX6 fusion construct) plasmids (kindly provided by Aron Fisher, University of Pennsylvania, Philadelphia, PA) by liposome transfection. The cells expressing GFP or PRDX6-GFP fusion proteins were incubated with H_2O_2 for 24 h.

Statistical Analysis. Statistical analyses were performed using two-tailed Student's *t* test and ANOVA as appropriate. $P < 0.05$ was considered statistically significant.

ACKNOWLEDGMENTS. We thank Erin L. Adams for editing the manuscript. Tissue 8-isoprostane levels were measured by the late Dr. Jason Morrow (Vanderbilt University, Nashville, TN) who died in 2008. We are very grateful for his contributions to our research. Anti-PRDX6 antibody and pEGFP-C1 and pEGFP-C1-PRDX6 plasmids were kindly provided by Dr. Aron Fisher (University of Pennsylvania, Philadelphia, PA). Anti-FKBP52 antibody and WT and *Fkbp52*$^{-/-}$ MEFs were kindly provided by Dr. Marc B. Cox (University of Texas, El Paso, TX). This study was supported in part by National Institutes of Health Grants HD12304 and DA006668. Y.H. is supported by the Japan Society for the Promotion of Science Postdoctoral Fellowships for Research Abroad. N.A. is supported by the 2214-Abroad Research Fellowship for PhD students from the Scientific and Technological Research Council of Turkey (TUBITAK).

1. Margalioth EJ, Ben-Chetrit A, Gal M, Eldar-Geva T (2006) Investigation and treatment of repeated implantation failure following IVF-ET. *Hum Reprod* 21:3036–3043.
2. Dey SK, et al. (2004) Molecular cues to implantation. *Endocr Rev* 25:341–373.
3. Lydon JP, et al. (1995) Mice lacking progesterone receptor exhibit pleiotropic reproductive abnormalities. *Genes Dev* 9:2266–2278.
4. Smith DF (2004) Tetratricopeptide repeat cochaperones in steroid receptor complexes. *Cell Stress Chaperones* 9:109–121.
5. Zhong L, et al. (2004) Heat-shock treatment-mediated increase in transduction by recombinant adeno-associated virus 2 vectors is independent of the cellular heat-shock protein 90. *J Biol Chem* 279:12714–12723.
6. Davies TH, Sánchez ER (2005) Fkbp52. *Int J Biochem Cell Biol* 37:42–47.
7. Mamane Y, Sharma S, Petropoulos L, Lin R, Hiscott J (2000) Posttranslational regulation of IRF-4 activity by the immunophilin FKBP52. *Immunity* 12:129–140.
8. Tranguch S, et al. (2005) Cochaperone immunophilin FKBP52 is critical to uterine receptivity for embryo implantation. *Proc Natl Acad Sci USA* 102:14326–14331.
9. Tranguch S, et al. (2007) FKBP52 deficiency-conferred uterine progesterone resistance is genetic background and pregnancy stage specific. *J Clin Invest* 117:1824–1834.
10. Manevich Y, Fisher AB (2005) Peroxiredoxin 6, a 1-Cys peroxiredoxin, functions in antioxidant defense and lung phospholipid metabolism. *Free Radic Biol Med* 38:1422–1432.
11. Phelan SA (1999) AOP2 (antioxidant protein 2): Structure and function of a unique thiol-specific antioxidant. *Antioxid Redox Signal* 1:571–584.
12. Wang X, et al. (2003) Mice with targeted mutation of peroxiredoxin 6 develop normally but are susceptible to oxidative stress. *J Biol Chem* 278:25179–25190.
13. Das SK, et al. (1994) Heparin-binding EGF-like growth factor gene is induced in the mouse uterus temporally by the blastocyst solely at the site of its apposition: A possible ligand for interaction with blastocyst EGF-receptor in implantation. *Development* 120:1071–1083.
14. Daikoku T, et al. (2005) Proteomic analysis identifies immunophilin FK506 binding protein 4 (FKBP52) as a downstream target of Hoxa10 in the periimplantation mouse uterus. *Mol Endocrinol* 19:683–697.
15. Kay JE (1996) Structure-function relationships in the FK506-binding protein (FKBP) family of peptidylprolyl cis-trans isomerases. *Biochem J* 314:361–385.
16. Ain R, Dai G, Dunmore JH, Godwin AR, Soares MJ (2004) A prolactin family paralog regulates reproductive adaptations to a physiological stressor. *Proc Natl Acad Sci USA* 101:16543–16548.
17. Hakim RB, Gray RH, Zacur H (1998) Alcohol and caffeine consumption and decreased fertility. *Fertil Steril* 70:632–637.
18. Howe G, Westhoff C, Vessey M, Yeates D (1985) Effects of age, cigarette smoking, and other factors on fertility: Findings in a large prospective study. *Br Med J (Clin Res Ed)* 290:1697–1700.
19. Ruder EH, Hartman TJ, Blumberg J, Goldman MB (2008) Oxidative stress and antioxidants: Exposure and impact on female fertility. *Hum Reprod Update* 14:345–357.
20. Wang H, et al. (2005) Variation in commercial rodent diets induces disparate molecular and physiological changes in the mouse uterus. *Proc Natl Acad Sci USA* 102:9960–9965.
21. Lim H, Ma L, Ma WG, Maas RL, Dey SK (1999) Hoxa-10 regulates uterine stromal cell responsiveness to progesterone during implantation and decidualization in the mouse. *Mol Endocrinol* 13:1005–1017.
22. Matsumoto H, Zhao X, Das SK, Hogan BL, Dey SK (2002) Indian hedgehog as a progesterone-responsive factor mediating epithelial-mesenchymal interactions in the mouse uterus. *Dev Biol* 245:280–290.
23. Fischer B, Bavister BD (1993) Oxygen tension in the oviduct and uterus of rhesus monkeys, hamsters and rabbits. *J Reprod Fertil* 99:673–679.
24. Dennery PA (2007) Effects of oxidative stress on embryonic development. *Birth Defects Res C Embryo Today* 81:155–162.
25. Nonogaki T, Noda Y, Narimoto K, Umaoka Y, Mori T (1991) Protection from oxidative stress by thioredoxin and superoxide dismutase of mouse embryos fertilized in vitro. *Hum Reprod* 6:1305–1310.
26. Wang X, et al. (2002) Vitamin C and vitamin E supplementation reduce oxidative stress-induced embryo toxicity and improve the blastocyst development rate. *Fertil Steril* 78:1272–1277.
27. Giudice LC, Kao LC (2004) Endometriosis. *Lancet* 364:1789–1799.
28. Augoulea A, Mastorakos G, Lambrinoudaki I, Christodoulakos G, Creatsas G (2009) The role of the oxidative-stress in the endometriosis-related infertility. *Gynecol Endocrinol* 25:75–81.
29. Hirota Y, et al. (2008) Deficiency of immunophilin FKBP52 promotes endometriosis. *Am J Pathol* 173:1747–1757.
30. Cheung-Flynn J, et al. (2005) Physiological role for the cochaperone FKBP52 in androgen receptor signaling. *Mol Endocrinol* 19:1654–1666.
31. Lydon JP, et al. (1995) Mice lacking progesterone receptor exhibit pleiotropic reproductive abnormalities. *Genes Dev* 9:2266–2278.
32. Lim H, et al. (1997) Multiple female reproductive failures in cyclooxygenase 2-deficient mice. *Cell* 91:197–208.
33. Noyes RW, Hertig AI, Rock J (1950) Dating the endometrial biopsy. *Fertil Steril* 1:3–25.
34. Hirota Y, et al. (2010) Uterine-specific p53 deficiency confers premature uterine senescence and promotes preterm birth in mice. *J Clin Invest* 120:803–815.
35. Morrow JD, Roberts LJ, 2nd (1999) Mass spectrometric quantification of F2-isoprostanes in biological fluids and tissues as measure of oxidant stress. *Methods Enzymol* 300:3–12.
36. Daikoku T, et al. (2007) Extracellular signal-regulated kinase is a target of cyclooxygenase-1-peroxisome proliferator-activated receptor-delta signaling in epithelial ovarian cancer. *Cancer Res* 67:5285–5292.

Supporting Information

Hirota et al. 10.1073/pnas.1009324107

SI Materials and Methods

2D-DIGE Analysis and Protein Identification. DeCyder v6.5 software (Amersham Biosciences) was used for simultaneous comparison of abundance changes across all 10 samples with statistical confidence. Data reduction by principle components analysis demonstrated that in *ca*. 100 intact protein features that changed significantly ($P < 0.01$, ANOVA) among these three genotypes across all samples, the major source of variation (PC1 = 63.5) separated the PR-null ($Pgr^{-/-}$) samples from the others, and the second greatest source of variation (PC2 = 24.4) separated the remainder of the samples by WT vs. FK506-binding protein 52-deficient ($Fkbp52^{-/-}$). These results provided additional confidence that the observed changes were reflective of the biology rather than arising from unanticipated experimental or biological variation. Proteins of interest were robotically excised and processed for MS analyses using an Ettan Spot Handling Workstation (GE Healthcare). MALDI-TOF MS and TOF/TOF tandem MS were performed on a Voyager 4700 (Applied Biosystems) using data-dependent tandem MS acquisition on the 20 most abundant ions in each MALDI-TOF peptide mass map. MALDI-TOF peptide mass maps and accompanying tandem mass spectra then were collectively searched against the Swiss-Prot and NCBInr databases using GPS Explorer software (Applied Biosystems) running the Mascot database search engine (Matrix-Science). Searches were performed without constraining protein molecular weight or isoelectric point and allowed for carbamidomethylation of cysteine, partial oxidation of methionine residues, and one missed trypsin cleavage. Identifications were accepted based on a tripartite evaluation that takes into account significant molecular weight search (MOWSE) scores, spectrum annotation, and observed vs. expected migration on the 2D gel (1).

1. Friedman DB, et al. (2004) Proteome analysis of human colon cancer by two-dimensional difference gel electrophoresis and mass spectrometry. *Proteomics* 4: 793–811.

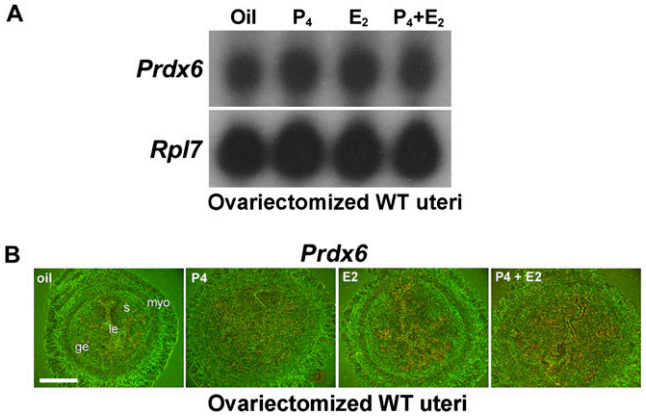


Fig. S1. Effects of progesterone (P_4) and/or estradiol-17β (E_2) on peroxiredoxin-6 (*Prdx6*) expression in ovariectomized WT uteri. (*A*) Expression levels of uterine *Prdx6* mRNA in ovariectomized CD1 WT mice treated with oil (vehicle), P_4, E_2, or P_4+E_2 for 24 h as determined by Northern hybridization. *Rpl7* was used as a loading control. (*B*) In situ hybridization showing differential patterns of *Prdx6* expression in ovariectomized CD1 WT uteri treated with oil, P_4, E_2, or P_4+E_2. ge, glandular epithelium; le, luminal epithelium; myo, myometrium; s, stroma. (Scale bar, 200 μm.)

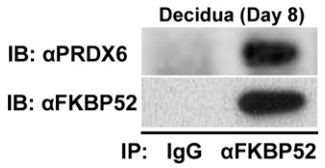


Fig. S2. Physical association of FK506-binding protein 52 (FKBP52) with PRDX6 in day 8 decidua. Decidual cell protein extracts were immunoprecipitated with an anti-FKBP52 antibody. Pulled-down complexes were run on SDS/PAGE and immunoblotted using antibodies specific to PRDX6 or FKBP52. The control immunoprecipitation (IP) was performed by incubating protein lysates with a rabbit IgG. IB, immunoblotting.

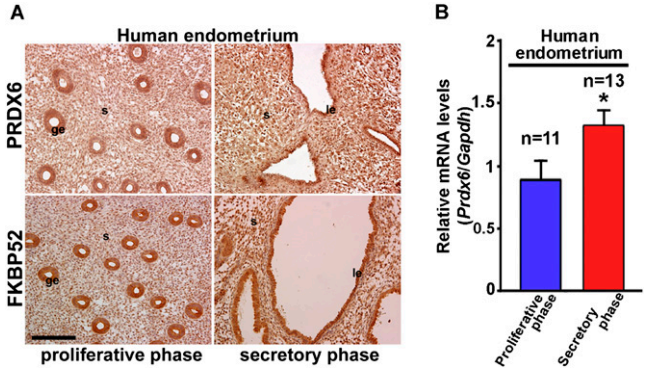


Fig. S3. PRDX6 expression in the human endometrium. (*A*) Immunostaining of PRDX6 and FKBP52 in human endometrium. Brown deposits indicate sites of positive immunostaining. ge, glandular epithelium; le, luminal epithelium; s, stroma. (Scale bar, 200 μm.) (*B*) Expression levels of *Prdx6* mRNA are higher in the secretory phase of human endometrium than in the proliferative phase. The number of samples assessed is indicated above each bar. Values are mean ± SEM. $*P < 0.05$.

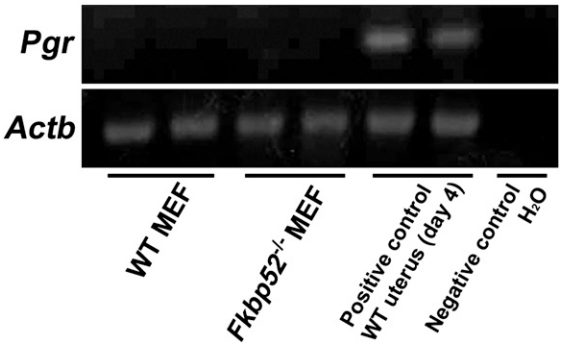


Fig. S4. Progesterone receptor (*Pgr)* mRNA is undetectable in mouse embryonic fibroblasts (MEFs). Undetectable levels of *Pgr* mRNA in WT and *Fkbp52*$^{-/-}$ MEFs as determined by RT-PCR. *Actb* served as an internal control. WT uteri at day 4 of pregnancy and water were used as positive and negative controls, respectively.

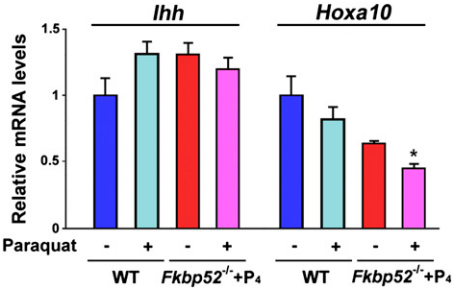


Fig. S5. Paraquat reduces *Hoxa10* expression in *Fkbp52*$^{-/-}$ uteri on day 4 of pregnancy. Expression levels of *Ihh* and *Hoxa10* mRNA in paraquat-treated uteri from WT and P_4-primed *Fkbp52*$^{-/-}$ mice on day 4 of pregnancy as determined by Northern hybridization are shown. Band intensities of *Ihh* and *Hoxa10* were normalized against *Rpl7*. *Fkbp52*$^{-/-}$ females were treated with P_4 (2 mg/d) on days 2–4 of pregnancy. Paraquat was injected on the evening (1800 hours) of day 3 of pregnancy. Two or three independent samples from different mice were examined in each group. Data are given as mean ± SEM. $*P < 0.05$ compared with P_4-primed *Fkbp52*$^{-/-}$ mice without paraquat.

Table S1. Proteins down-regulated selectively in *Fkbp52*$^{-/-}$ uteri

Protein identification	Accession number	MW pl	WT vs. *Pgr*$^{-/-}$ Av ratio	WT vs. *Pgr*$^{-/-}$ *P* (*t* test)	WT vs. *Fkbp52*$^{-/-}$ Av ratio	WT vs. *Fkbp52*$^{-/-}$ *P* (*t* test)	*Pgr*$^{-/-}$ vs. *Fkbp52*$^{-/-}$ Av ratio	*Pgr*$^{-/-}$ vs. *Fkbp52*$^{-/-}$ *P* (*t* test)	*P* (ANOVA)
FK506-binding protein 52 (FKBP52)	P30416	51.8 5.5	1.04	0.75	−3.62	0.0005	−3.77	0.0004	0.00006
Peroxiredoxin-6 (PRDX6)	O008709	24.8 5.7	1.01	0.77	−2.01	0.04	−2.02	0.00004	0.036

Accession numbers in Swiss-Prot database were used. Theoretical molecular weight (MW, in kDa) and isoelectric point (pl) are calculated from the database entries, which often contain precursor sequences not present in the mature form migrating on the gel. Average volume ratios (Av ratio) and *P* values of Student's *t* test and ANOVA were calculated using DeCyder software version 6.5, using mixed-sample internal standard methodology.

Table S2. Proteins up-regulated selectively in *Fkbp52*$^{-/-}$ uteri

Protein identification	Accession number	MW pl	WT vs. *Pgr*$^{-/-}$ Av ratio	WT vs. *Pgr*$^{-/-}$ *P* (*t* test)	WT vs. *Fkbp52*$^{-/-}$ Av ratio	WT vs. *Fkbp52*$^{-/-}$ *P* (*t* test)	*Pgr*$^{-/-}$ vs. *Fkbp52*$^{-/-}$ Av ratio	*Pgr*$^{-/-}$ vs. *Fkbp52*$^{-/-}$ *P* (*t* test)	*P* (ANOVA)
Vimentin	P20152	53.5 5.1	1.00	0.93	1.28	0.017	1.28	0.005	0.008
Desmin	P31001	53.3 5.2	1.02	0.90	1.33	0.008	1.31	0.031	0.016
Aldehyde dehydrogenase, mitochondrial precursor	P47738	57.0 7.5	1.05	0.50	1.26	0.005	1.20	0.005	0.005
Eukaryotic initiation factor 4A-1	P29562	45.4 5.3	−1.03	0.79	1.19	0.028	1.22	0.003	0.016
Charged multivesicular body protein 2a	Q9DB34	25.1 5.9	−1.00	0.97	1.36	0.006	1.36	0.006	0.002
Indolethylamine N-methyltransferase	P40936	30.0 6.0	1.08	0.73	2.39	0.01	2.21	0.013	0.008